Journal Name

ARTICLE

pH-Triggered Self-assembly and Hydrogelation of Cyclic Peptide Nanotubes Confined in Water Micro-droplets

Received 00th January 20xx,

Accepted 00th January 20xx

DOI: 10.1039/x0xx00000x

www.rsc.org/

Alejandro Méndez-Ardoy,[1] Juan R. Granja[1]* and Javier Montenegro[1]*

The controlled one-dimensional supramolecular polymerization of synthetic building blocks in confined spaces constitutes a key challenge to simplify the understanding of the fundamental physical principles behind the behavior of more complex encapsulated polymer networks. Cyclic peptide nanotubes constitute an optimal scaffold for the fabrication of hierarchical one-dimensional self-assembled architectures. Herein we report the pH-controlled nanotube formation and fibrillation of supramolecular cyclic peptides in confined aqueous droplets. The externally triggered self-assembly of these peptides gave rise to viscoelastic hydrogels in which the one-dimensional molecular arrangement was perfectly preserved from the nano- to the micro-scale. The cyclic peptides building blocks were confined inside water microdroplets and the base-triggered supramolecular polymerization was externally triggered and followed by confocal microscopy showing that the confined fibrillation spanned and affected the shape of the droplet micro container.

Introduction

Hierarchical self-assembly of molecular entities and hydrogelation in confined spaces are ubiquitous processes in nature.[1] The progress of supramolecular chemistry has developed a plethora of building blocks capable of assembling into nanotubular structures.[2-13] The strong interest and the importance of confining one-dimensional self-assembly processes has triggered several pioneering strategies from different research groups.[14-22] These recent studies have shown the importance of synthetic chemistry to provide innovative small molecules that can give rise to precise supramolecular architectures with improved properties. Along these lines, the pH-triggered self-assembly[23] of peptides and polymers has been recently exploited for the preparation of tubular folded ensembles[12,24] and for the development of cooperative supramolecular polymeric sensors.[25] Therefore, there is a strong and growing demand for simple and yet functional materials that could mimic the hierarchical self-assembly of more complex natural nano- and micro-fibers. These artificial building blocks would provide a new set of synthetic tools that could contribute to the understanding of the physical properties of well-defined fibrillated networks inside confined spaces. Furthermore, the development of stimuli-responsive synthetic tubular structures which can be externally assembled in confined spherical micro-volumes, may open up new possibilities for material sciences and synthetic biology. In this regard, cyclic peptides of alternating chirality constitute optimal scaffolds for the preparation of nanotubes with controlled diameter, external decoration and chemical properties.[26,27]

Herein we report the design, synthesis and characterization of droplet-confined cyclic peptides that polymerize into nanotubes after the external addition of base. The cyclic peptide, equipped with two imidazole moieties (His), showed a cooperative deprotonation mechanism and a subsequent organization into a hierarchical architecture. The resulting microfibrillated hydrogel exhibited an elastic behaviour with a perfect preservation of the one-dimensional arrangement from the molecular level to the micro scale. The fibrillation process was externally controlled within the confined spherical micro-volume of the water droplets. The synthetic microtubules spanned the inner cavity of the water droplets, which showed a distorted spherical shape as a result of the confined fibrillation process. The methodology described here provides new materials made of simple and robust cyclic peptides that offer control over the diameter and the chemical functions of the self-assembled architecture.

Cyclic peptide **CP1** (Scheme 1) was prepared by Fmoc solid phase peptide synthesis as illustrated in Scheme S1-S2 in the supporting information.[28] The alternating chirality of this octapeptide predisposes the amide bonds perpendicular to the peptide plane to ring stack by the formation of

[a] Centro Singular de Investigación en Química Biolóxica e Materiais Moleculares (CIQUS), Departamento de Química Orgánica, Universidade de Santiago de Compostela, 15782 Santiago de Compostela, Spain. *e-mail: juanr.granja@usc.es, javier.montenegro@usc.es

Electronic Supplementary Information (ESI) available: [details of any supplementary information available should be included here]. See DOI: 10.1039/x0xx00000x

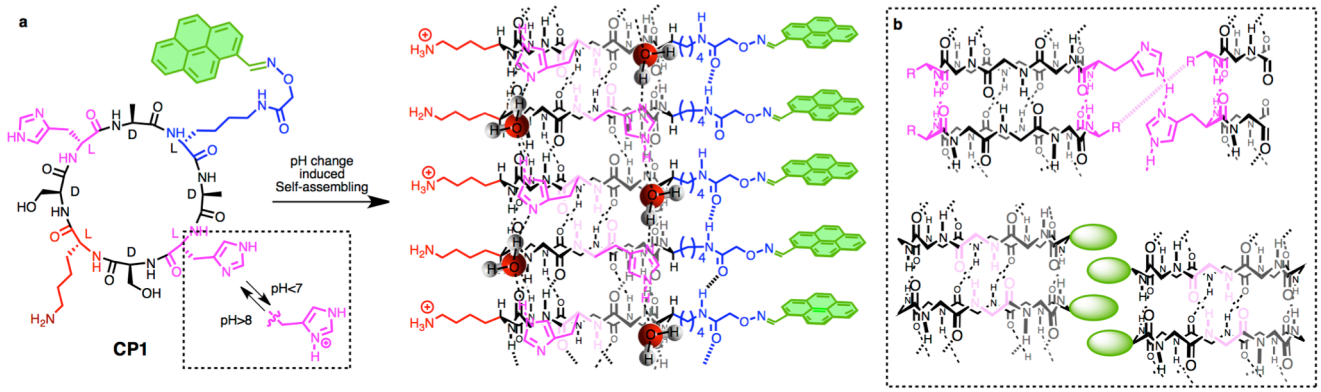

Scheme 1. a) Structure and self-assembly of **CP1** in single peptide nanotubes. b) Single peptide nanotubes can further aggregate for hierarchical micro-fibrillation by histidine hydrogen-bonded networks and pyrene π-stacking and hydrophobic effects.

hydrogen-bonded antiparallel β-sheets (Scheme 1). In this regard, the amino acid side chains are radially exposed along the nanotube longitudinal axis.[29] The cyclic peptide sequence included three pH sensitive residues (His and Lys) and one alcoxyamine residue that was introduced to tune the peptide hydrophobicity by oxime conjugation with aldehydes such as pyrene-1-carbaldehyde.[28,30-32] This amphiphilic architecture was selected to give rise to self-assembled nanotubes that could further interact by the formation of water assisted histidine-histidine hydrogen bonds[33], hydrophobic, π-π and/or cation-π interactions.[28] **CP1** presented self-assembling properties as shown by the pH dependent emission of pyrene excimer caused by the stacking of the aromatic fluorophore (Fig. 1).

The neutralization of the aqueous media gave rise to the deprotonation of the histidine side chains that triggered the supramolecular events denoted by the quenching and the shift of the fluorescence of the emission band towards the pyrene excimer at 470 nm (Fig. 1a and S1).[28,35] In the final nanotube ensemble, at pH above 8, the Lys side chains could be deprotonated to minimize the cationic electrostatic repulsions (Scheme 1).[34] The formation of the putative antiparallel β-sheets on the dried gel was confirmed by the infrared bands of the amides I and II at 1623 and 1538 cm^{-1} respectively (Fig. S2).[36] Fluorescence experiments in the presence of thioflavin T (ThT) further supported the antiparallel β-sheet arrangement,[37] as the alkalinization-triggered self-assembly of **CP1** lead to the expected increase of the emission of the mechanosensitive fluorophore ThT (Fig. S3). Circular dichroism titrations at different concentrations gave a rough estimation of association constants of 4 x 10^6 M^{-1} (at pH 8, Fig. S5).[38] UV titrations revealed that the hypsochromic shift of the pyrene absorption bands at 350 and 290 nm are due to a potential change in the aggregated state of the nanotubes (Fig. S4).[23]

Circular dichroism (CD) of aqueous solution of **CP1** at pH 8 showed positive Cotton effects and a bisignate Cotton effect for the π → π* transition of pyrene, which confirms the transfer of chirality from the peptide backbone to the chromophore (Fig. 1b and S5). The plot of the CD maximum (360 nm) against the pH (Fig. 1c) provided mean values of *p*Ka = 6.0 ± 0.4 and a Hill coefficient of *n* = 3.3 ± 1.8 (Hill equation).[25] The observed sharp transition suggested the requirement of monomer deprotonation and a cooperative mechanism for the peptide self-assembly.[25]

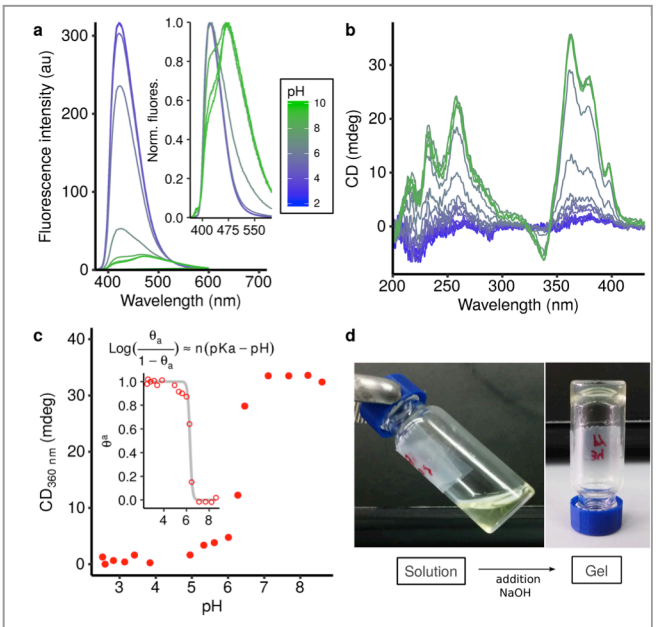

Figure 1. pH-triggered self-assembly of **CP1** in water: a) Fluorescence emission at different pH of **CP1** (200 μM) in water (λ_{ex} = 340 nm). Inset: normalized fluorescence emission at maximum emission. b) CD spectra of **CP1** (400 μM) in water at different pH. c) CD signal at 360 nm against the pH. Inset shows the fitting to a Hill model. d) 2% w/w solution of **CP1** in milliQ water before (left) and after (right) addition of NaOH (0.1 M) to pH ~ 8-9.

Addition of small aliquots of sodium hydroxide to acidic solutions of **CP1** (2% weight) triggered nanotube assembly and gelation of the aqueous environment as shown by the vial inversion test (Fig. 1d). Deposition of diluted hydrogel aliquots, on top of mica surfaces, revealed the presence of networks of nanotubes with heights of 2.5-3.0 nm, which matched with the diameter of **CP1** (Fig. 2a and Fig. S6-7). The persistence length obtained by AFM analysis was around 5 µm, which is similar to that of actin and intermediate filaments.[39] Transmission electron microscopy (STEM and TEM) micrographs confirmed the presence of single peptide nanotubes (3 nm), bundles of nanotubes (6-10 nm) and entangled peptide nanotubular networks (Fig. 2b, Fig. S8). We next employed Laser Scanning Confocal Microscopy (LSCM) to study the arrangement of the peptide hydrogel at the micrometer scale (Fig. 2c). Analysis of the planes close to the gel-glass interface showed that the hierarchical architecture was preserved from the nanotubes to fibers with contour lengths of tens of micrometers.[40] The elastic properties of the gel were obtained by measuring the response of the material to a shear deformation (Fig. 2d).[41,42] Strain tests showed a linear viscoelastic region below 10% strain. Frequency sweeps at constant strains of 5% showed that *G*' was about 3 times larger than *G*'', revealing a gel with elastic behaviour that can accumulate mechanical energy (Fig. 2d).[41]

Peptide self-assembly experiments were next carried out in water in oil droplets to investigate the externally induced supramolecular polymerization in confined spaces (Fig. 3). Water droplets containing **CP1** at approximately pH 4 were prepared by emulsification method.[43] Aqueous solution of **CP1** was added to heavy mineral oil containing egg yolk phosphatidylcholine, the mixture was stirred until a white emulsion was formed and the droplets were ready for microscopy observation. The glass microscope slides were fluorinated to prevent the collapse of the droplet on top of the glass surface (see supporting info). Two strategies were employed to study nanotube formation and fibrillation within water microdroplets (Fig. 3, ii and iii). In the *pre-formation* small volumes of **CP1** aqueous solutions were diluted with HEPES buffer (pH 8) and subsequently submitted to the droplet formation (Fig. 3-ii). In the second strategy, *in situ*, water droplets containing freshly prepared acidic suspensions of **CP1** were treated with propanamine, which is a base soluble in both water and oil media (Fig. 3, iii).[43] Epifluorescence and confocal microscopy images of the acidic droplets suspensions showed uniform pyrene blue fluorescence, suggesting that droplet-confined **CP1** remains in the aqueous phase in a non-aggregated state and homogeneously distributed (Fig. 3a-i). However, pre-dilution of **CP1** with HEPES (pH 8) and subsequent droplet formation caused the bathochromic shift of the droplet fluorescence and the formation of confined fibril-like structures of several microns in length (Fig. 3-ii, Fig. S10). This "*green-shifted*" emission correlates with the observed excimer emission of pyrene (Fig. 1a). Acidic droplets of **CP1** were then employed to study the externally induced self-assembly in confined media (Fig. 3-iii, Fig. 4, Fig. 5). Addition of propanamine to suspensions of these droplets triggered peptide self-assembly and fiber formation. Confocal microscopy images of the basified droplets (HEPES or propanamine) showed the presence of micrometer sized 1D fibril-like structures that transversally spanned the droplets inner volume (Fig. 3). In situ experiments confirmed that fibrillation occurred immediately after propanamine addition.

Confined peptide self-assembly was next carried out in the presence of the hydrophilic fluorophore (rhodamine) to confirm the integrity of the fibrillated droplets. The micrographs confirmed the homogenous distribution of the red dye in both acidic and fibrillated droplets (Fig. 4a-d). The droplet fibrillation process triggered by propanamine was confirmed to take place without droplet disruption (Fig. 4e-f). In these experiments, droplets were observed in the fluorescence microscope after the local addition of the base in one side of the incubation chamber. Intriguingly, the corresponding micrographs exhibited a pH gradient-dependent, stimuli-responsive fibrillation process. Droplets in close proximity to the local addition point showed the corresponding "*green shift*" and fibrillation patterns. On the other hand, droplets far from the addition zone remained "*blue*" and with homogenously dispersed cyclic peptides (Fig. 4d).

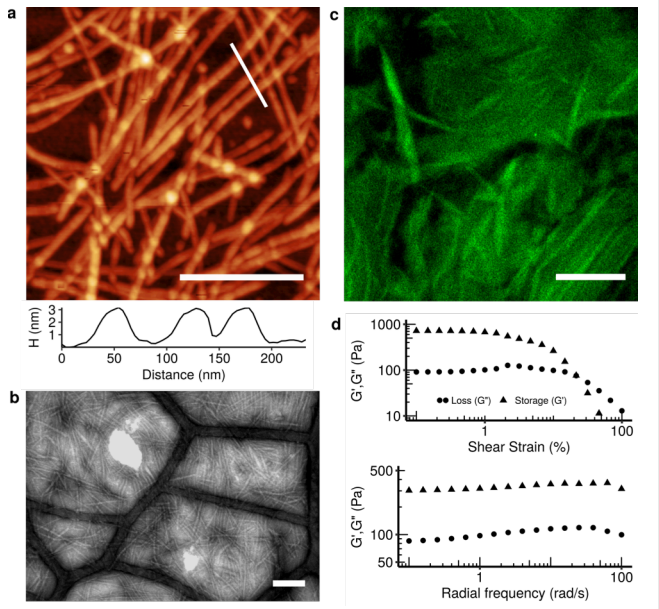

Figure 2. Peptide nanotubes at different length scales (nano to micro). a) AFM micrographs of **CP1** (1.8 mM, pH 8) on mica substrates. The height profile was obtained along the white line shown in the image. b) STEM micrographs on formvar/carbon grids (180 µM, pH 8). c) Section of LSCM images of gels after basification of **CP1** (2% w/w) with NaOH 0.1 M. Scale bars correspond to 400 nm (a), 100 nm (b) and 20 µm (c). d) Rheology measurements for gels of **CP1** (2% w/w): strain test and frequency sweep at constant strain of 5%.

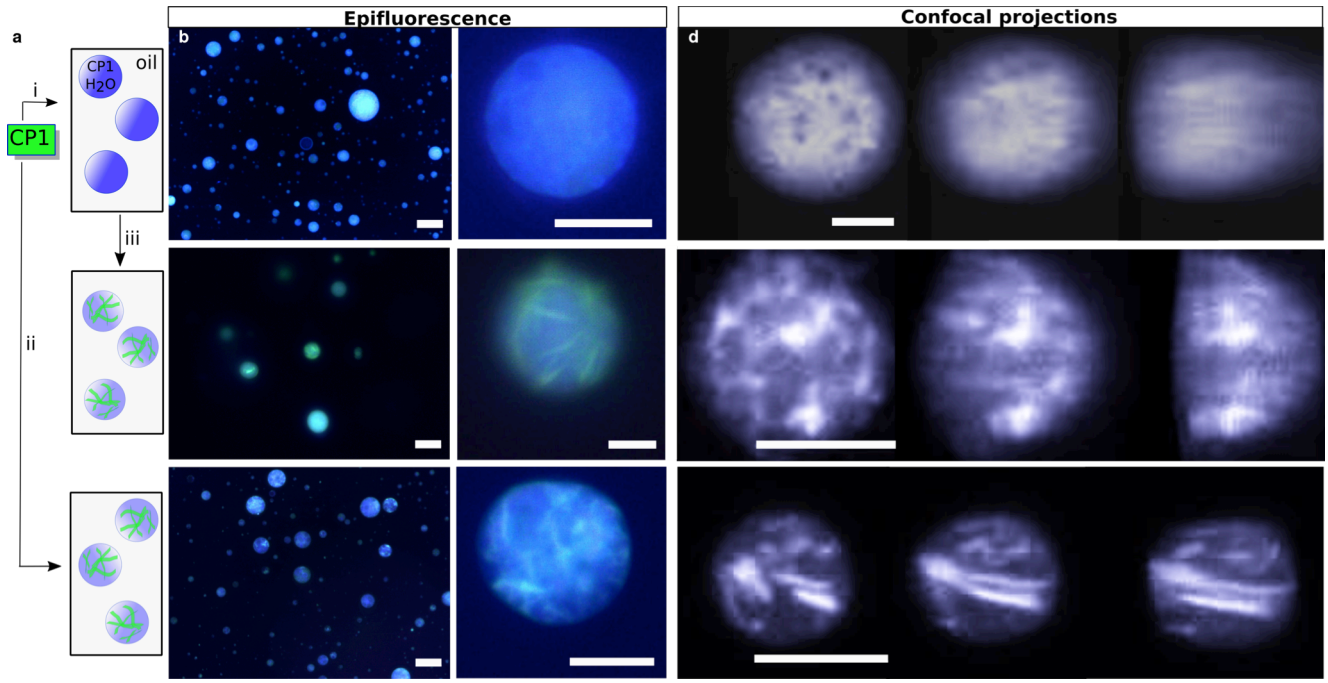

Figure 3. Supramolecular polymerization of **CP1** in confined spaces. a) Scheme of the procedure for the formation of fibers within water-in-oil droplets: i) **CP1** in water (1-2% w/w); ii) **CP1** (1-2% w/w) in HEPES 30 mM at pH 8; iii) addition of propanamine b) Epifluorescence images of droplets at low magnification. c) Epifluorescence images of individual droplets at high magnification. d) Confocal microscopy projections of individual droplets. Scale bars are 20 µm for b) 5 µm for c) and 10 µm for d).

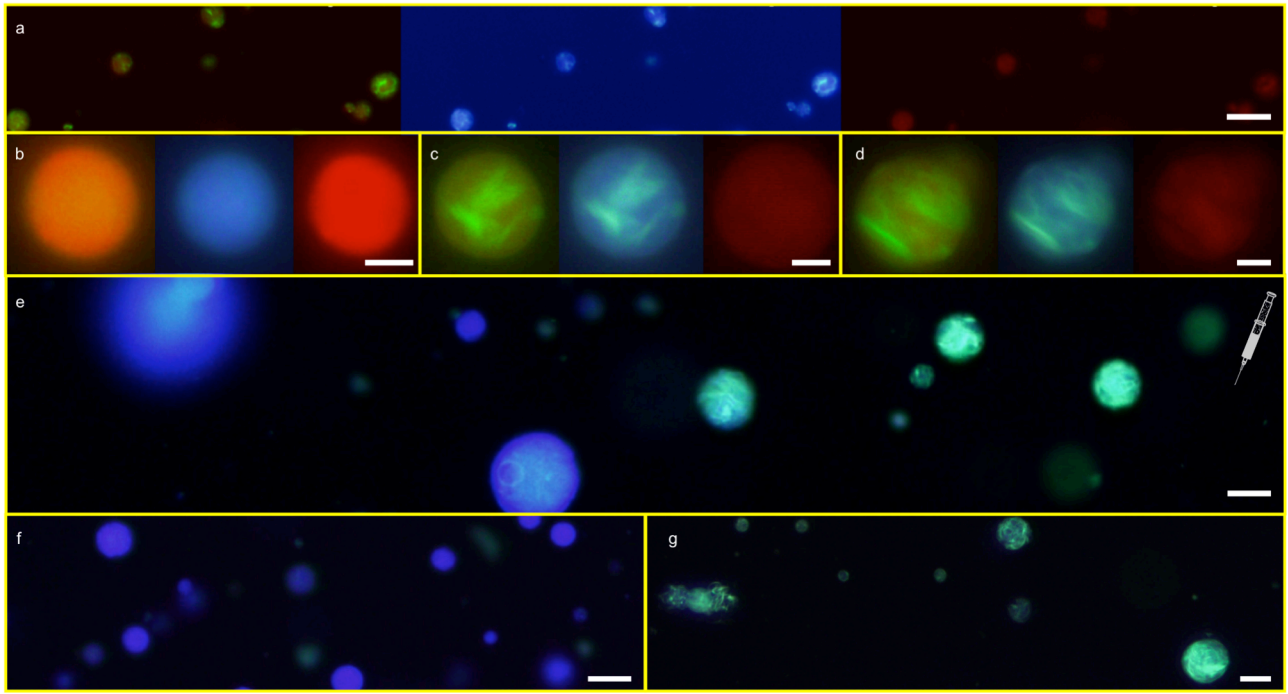

Figure 4. a), b), c), d) Fibrillation in rhodamine-containing droplets. Merged channels (left), pyrene channel (middle) and rhodamine channel (right). a) Pre-fibrillation triggered by dilution in HEPES buffer (pH ~ 8). b) Detail of the control experiments of aqueous droplets at acidic pH (~ 4). c) Detail of a preformed fibrillated droplet by HEPES (pH ~ 8) dilution. d) Detail of an *in situ* fibrillated droplet by addition of propanamine. e) Micropipette local addition of propanamine from the top right corner of the micrograph-triggered the "*green-shift*" and the fibrillation process in a gradient dependent fashion. f) Detail of droplets far from propanamine addition. g) Detail of droplets nearby the propanamine addition. Scale bars are 5 µm for b), c) and d) and 20 µm for a) e), f) and g).

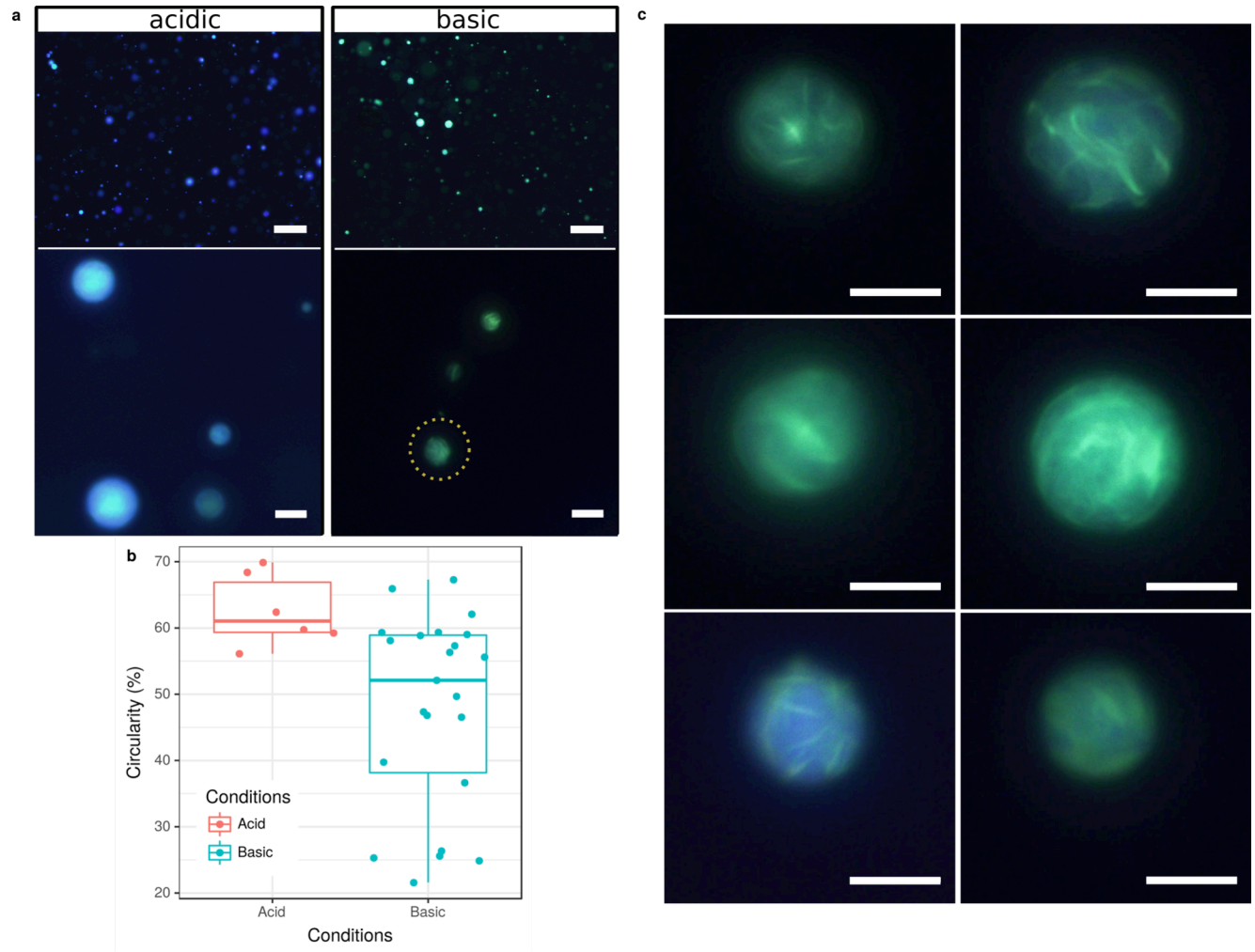

Figure 5. Peptide fibrillation in water-in-oil emulsions of **CP1** (2% w/w); a) before (left) and after (right) addition of propanamine (1% v/v in oil). Yellow dotted line highlight loss of circularity in droplets containing nanotubes; b) Boxplot and experimental points comparing circularity in both conditions determined by image analysis with Image J; c) Details of droplets showing fibers of micrometre size. In all cases scale bar is 10 μm.

As previously reported for other droplet-confined materials,[40] the peptide-fibrillated droplets reported here exhibited a distorted spherical shape with protrusions and heterogeneous contours that could be observed after the supramolecular polymerization (Fig. 3c and 4g). This distorted shape of the fibrillated droplets was statistically confirmed by the boxplot of the experimental points comparing the circularity of the droplets in both conditions (Fig. 5).

In summary, we have introduced peptide nanotubes as excellent scaffolds for the network fibrillation in confined spaces. The resulting architectures were reminiscent of more complex natural pH-modulated mechanotransduction systems.[44] The high persistent length of nanotubes reported here (~ 5 μm) could be related with the subsequent strong directionality of the supra-assembly that afforded microfibers with contour lengths of tens of micro-meters.[40] This pH-triggered self-assembly strategy afforded confined fibrillated networks that allowed tracking of the self-assembly process by fluorescence microscopy. The confined fibrillation caused the deformation of the droplet containers confirming that confined supramolecular polymerization influences the container shape. The development of simple and accessible stimuli-responsive materials that can be confined and hierarchically assembled in one-dimension, from the nano to the micro scale, could allow a better physical understanding of the mechanisms that underline well-defined more complex composite tubular networks inside discrete environments. The simple cyclic peptide materials reported here can be prepared by straightforward synthetic procedures and they provide a full control over the assembly process, tube diameter, external decoration and the chemical properties of the resulting tubular ensemble. Furthermore, the results reported here could lead to potential applications for multivalent presentation of biological motifs for tissue engineering as well as pH sensitive biomaterials for controlled drug release. The robust preservation of the one-dimensional self-assembly in confine

spaces, from the nano- to the micro-scale, could also contribute to the development of new materials for bottom up approaches in synthetic biology.

Acknowledgements

We thank Carmen Alvarez and Carlos García (USC) for their assistance with rheology. This work was partially supported by the Spanish Agencia Estatal de Investigación (AEI) [SAF2017-89890-R, CTQ2014-59646-R and CTQ2016-78423-R], the Xunta de Galicia (ED431G/09, ED431C 2017/25 and 2016-AD031) and the ERDF. A. M-A. received a M.C.I.F. from the EC (GLYCONANOPEP-750248). J.M. holds a Ramón y Cajal (RYC-2013-13784), an ERC-Stg (DYNAP-677786) and a Young Investigator Grant from the HFSP (RGY0066/2017).

References

1 J.-F. Joanny and J. Prost, *HFSP Journal*, 2009, **3**, 94–104.
2 D. Bong, T. Clark, J. Granja and M. Ghadiri, *Angew. Chem. Int. Ed.*, 2001, **40**, 988–1011.
3 A. Fuertes, J. Marisa, J. R. Granja and J. Montenegro, *Chem. Commun.*, 2017, **53**, 7861–7871.
4 E. Krieg, M. M. C. Bastings, P. Besenius and B. Rybtchinski, *Chem. Rev.*, 2016, **116**, 2414–2477.
5 J. Boekhoven, W. E. Hendriksen, G. J. M. Koper, R. Eelkema and J. H. van Esch, *Science*, 2015, **349**, 1075–1079.
6 J. Boekhoven, A. M. Brizard, M. C. A. Stuart, L. Florusse, G. Raffy, A. Del Guerzo and J. H. van Esch, *Chem. Sci.*, 2016, **7**, 6021–6031.
7 A. Sorrenti, J. Leira-Iglesias, A. J. Markvoort, T. F. A. De Greef and T. M. Hermans, *Chem. Soc. Rev.*, 2017, **46**, 5476–5490.
8 A. Sorrenti, J. Leira-Iglesias, A. Sato and T. M. Hermans, *Nat. Commun.*, 2017, 8:15899.
9 P. Besenius, G. Portale and P. Bomans, *Proc. Natl. Acad. Sci. U. S. A.*, 2010, **107**, 17888–17893.
10 D. Spitzer, L. L. Rodrigues, D. Straßburger, M. Mezger and P. Besenius, *Angew. Chem. Int. Ed.*, 2017, **56**, 15461–15465.
11 J. Boekhoven, J. M. Poolman, C. Maity, F. Li, L. van der Mee, C. B. Minkenberg, E. Mendes, J. H. van Esch and R. Eelkema, *Nat. Chem.*, 2013, **5**, 433–437.
12 R. Otter, K. Klinker, D. Spitzer, M. Schinnerer, M. Barz and P. Besenius, *Chem. Commun.*, 2018, **54**, 401–404.
13 J. W. Fredy, A. Méndez-Ardoy, S. Kwangmettatam, D. Bochicchio, B. Matt, M. C. A. Stuart, J. Huskens, N. Katsonis, G. M. Pavan and T. Kudernac, *Proc. Natl. Acad. Sci. U. S. A.*, 2017, **114**, 11850–11855.
14 R. Krishna Kumar, X. Yu, A. J. Patil, M. Li and S. Mann, *Angew. Chem. Int. Ed.*, 2011, **50**, 9343–9347.
15 A. Levin, T. C. T. Michaels, L. Adler-Abramovich, T. O. Mason, T. Müller, B. Zhang, L. Mahadevan, E. Gazit and T. P. J. Knowles, *Nat. Phys.*, 2016, **12**, 926–930.
16 R. K. Kumar, M. Li, S. N. Olof, A. J. Patil and S. Mann, *Small*, 2012, **9**, 357–362.
17 X. Huang, A. J. Patil, M. Li and S. Mann, *J. Am. Chem. Soc.*, 2014, **136**, 9225–9234.
18 D. S. Ferreira, R. L. Reis and H. S. Azevedo, *Soft. Matter.*, 2013, **9**, 9237–9248.
19 H.-K. Lee, S. Soukasene, H. Jiang, S. Zhang, W. Feng and S. I. Stupp, *Soft. Matter.*, 2008, **4**, 962–964.
20 S. Bai, S. Debnath, K. Gibson, B. Schlicht, L. Bayne, M. Zagnoni and R. V. Ulijn, *Small*, 2013, **10**, 285–293.
21 S. Mytnyk, A. G. L. Olive, F. Versluis, J. M. Poolman, E. Mendes, R. Eelkema and J. H. van Esch, *Angew. Chem. Int. Ed.*, 2017, **56**, 14923–14927.
22 S. A. P. van Rossum, M. Tena-Solsona, J. H. van Esch, R. Eelkema and J. Boekhoven, *Chem. Soc. Rev.*, 2017, **46**, 5519–5535.
23 B. Baumeister, A. Som, G. Das, N. Sakai, F. Vilbois, D. Gerard, S. P. Shahi and S. Matile, *Helv. Chim. Acta.*, 2002, **85**, 2740–2753.
24 H. Frisch, D. Spitzer, M. Haase, T. Basché, J. Voskuhl and P. Besenius, *Org. Biomol. Chem.*, 2016, **14**, 5574–5579.
25 Y. Li, T. Zhao, C. Wang, Z. Lin, G. Huang, B. D. Sumer and J. Gao, *Nat. Commun.*, 2016, 7:13214.
26 M. R. Ghadiri, J. R. Granja, R. A. Milligan, D. E. McRee and N. Khazanovich, *Nature*, 1993, **366**, 324–327.
27 J. D. Hartgerink, J. R. Granja, R. A. Milligan and M. R. Ghadiri, *J. Am. Chem. Soc.*, 1996, **118**, 43–50.
28 J. Montenegro, C. Vázquez-Vázquez, A. Kalinin, K. E. Geckeler and J. R. Granja, *J. Am. Chem. Soc.*, 2014, **136**, 2484–2491.
29 J. Montenegro, M. R. Ghadiri and J. R. Granja, *Acc. Chem. Res.*, 2013, **46**, 2955–2965.
30 J. Montenegro, E.-K. Bang, N. Sakai and S. Matile, *Chem. Eur. J.*, 2012, **18**, 10436–10443.
31 J. M. Priegue, J. Montenegro and J. R. Granja, *Small*, 2014, **10**, 3613–3618.
32 M. Pazo, H. Fernández-Caro, J. M. Priegue, I. Lostale Seijo and J. Montenegro, *Synlett*, 2017, **28**, 924–928.
33 I. G. Shenderovich, S. B. Lesnichin, C. Tu, D. N. Silverman, P. M. Tolstoy, G. S. Denisov and H.-H. Limbach, *Chem. Eur. J.*, 2015, **21**, 2915–2929.
34 G. Gasparini, E.-K. Bang, J. Montenegro and S. Matile, *Chem. Commun.*, 2015, **51**, 10389–10402.
35 M. Cuerva, R. Garcia-Fandino, C. Vázquez-Vázquez, M. A. López-Quintela, J. Montenegro and J. R. Granja, *ACS Nano*, 2015, **9**, 10834–10843.
36 H. S. Kim, J. D. Hartgerink and M. R. Ghadiri, *J. Am. Chem. Soc.*, 1998, **120**, 4417–4424.
37 L. S. Wolfe, M. F. Calabrese, A. Nath, D. V. Blaho, A. D. Miranker and Y. Xiong, *Proc. Natl. Acad. Sci. U. S. A.*, 2010, **107**, 16863–16868.
38 *This estimated association constant assumes that all the different interaction processes equally contribute to the nanotube formation.*
39 A. R. Bausch and K. Kroy, *Nat. Phys.*, 2006, **2**, 231–238.
40 M. M. A. E. Claessens, R. Tharmann, K. Kroy and A. R. Bausch, *Nat. Phys.*, 2006, **2**, 186–189.
41 M. L. Gardel, K. E. Kasza, C. P. Brangwynne, J. Liu and D. A. Weitz, in *Methods in Cell Biology*, Elsevier, 2008, vol. 89, pp. 487–519.
42 R. G. Weiss, *J. Am. Chem. Soc.*, 2014, **136**, 7519–7530.
43 S. Mashaghi and A. M. van Oijen, *Sci. Rep.*, 2015, 5:11837.
44 K. M. Schmoller, S. Köhler, A. H. Crevenna, R. Wedlich-Söldner and A. R. Bausch, *Soft. Matter.*, 2012, **8**, 9685–9690.

TOC